

## Exclusive $\eta$ production in pp reactions

I. Fröhlich<sup>1,a</sup>, F. Balestra<sup>2</sup>, Y. Bedfer<sup>3,b</sup>, R. Bertini<sup>2,3</sup>, L.C. Bland<sup>4</sup>, A. Brenschede<sup>1,c</sup>, F. Brochard<sup>3,d</sup>, M.P. Busa<sup>2</sup>, Seonho Choi<sup>4,e</sup>, M.L. Colantoni<sup>2</sup>, R. Dressler<sup>6,f</sup>, M. Dzemidzic<sup>4,d</sup>, J.-Cl. Faivre<sup>3,b</sup>, A. Ferrero<sup>2</sup>, L. Ferrero<sup>2</sup>, J. Foryciarz<sup>9,5,g</sup>, V. Frolov<sup>7</sup>, R. Garfagnini<sup>2</sup>, A. Grasso<sup>2</sup>, S. Heinz<sup>2,3</sup>, W.W. Jacobs<sup>4</sup>, W. Kühn<sup>1</sup>, A. Maggiora<sup>2</sup>, M. Maggiora<sup>2</sup>, A. Manara<sup>2,3</sup>, D. Panzieri<sup>8</sup>, H.-W. Pfaff<sup>1,h</sup>, G. Piragino<sup>2</sup>, A. Popov<sup>7</sup>, J. Ritman<sup>1</sup>, P. Salabura<sup>5</sup>, V. Tchalyshhev<sup>7</sup>, F. Tosello<sup>2</sup>, S.E. Vigdor<sup>4</sup>, and G. Zosi<sup>2</sup>

<sup>1</sup> II. Physikalisches Institut, University of Gießen, Gießen, Germany

<sup>2</sup> Dipartimento di Fisica “A. Avogadro” and INFN, Torino, Italy

<sup>3</sup> Laboratoire National Saturne, CEA Saclay, France

<sup>4</sup> Indiana University Cyclotron Facility, Bloomington, Indiana, USA

<sup>5</sup> M. Smoluchowski Institute of Physics, Jagellonian University, Kraków, Poland

<sup>6</sup> Forschungszentrum Rossendorf, Germany

<sup>7</sup> JINR, Dubna, Russia

<sup>8</sup> Università del Piemonte Orientale and INFN, Torino, Italy

<sup>9</sup> H. Niewodniczanski Institute of Nuclear Physics, Kraków, Poland

Received: 30 September 2002 /

Published online: 22 October 2003 – © Società Italiana di Fisica / Springer-Verlag 2003

**Abstract.** Angular distributions for the exclusive reaction  $pp \rightarrow pp\eta$  observed via the  $\pi^+\pi^-\pi^0$  decay channel have been measured at  $T_{\text{beam}} = 2.15$  GeV, 2.50 GeV and 2.85 GeV (excess energies  $Q = 324$  MeV, 412 MeV and 554 MeV). The polar angle of the  $\eta$  shows an anisotropy with respect to the beam direction for the lowest energy, which vanishes for the higher energies. The anisotropy of the  $pp$  polar angle increases slightly with the beam energy.

**PACS.** 13.75.Cs Nucleon-nucleon interactions (including antinucleons, deuterons, etc.) – 14.40.Aq  $\pi$ ,  $K$ , and  $\eta$  mesons – 25.40.Ve Other reactions above meson production thresholds (energies  $> 400$  MeV)

### 1 Introduction

The production of  $\eta$ -mesons in nucleon-nucleon collisions plays a role in elementary hadron physics to test various production models based on one-boson exchange [1–5]. In contrast to pion production,  $\eta$  production is dominated by the near-threshold resonance  $S_{11}(1535)N^*$ , which has a large coupling to the  $\eta$ -decay. Moreover, differential and total cross-section distributions measured in elementary  $\eta$  production are important for heavy-ion physics, where they are folded into model calculations. In nucleon-

nucleon collisions,  $\eta$  production has been measured in early bubble chamber experiments with sufficient statistic for total cross-sections and in near-threshold experiments with differential cross-section distributions up to a beam energies of 1.5 GeV [6–12], where the small phase space covers only a fraction of the  $S_{11}(1535)N^*$  signal.

In ref. [12], angular distributions of the  $\eta$ -meson in the Center-of-Mass system (CM) as well as for the  $pp$  system have been presented at near-threshold energies (excess energies 16 and 37 MeV). It has been shown that the distribution of the  $\eta$  CM polar angle ( $\cos\theta_{\eta}^{\text{CM}}$ ) is not isotropic and has a maximum flow of  $\eta$ -mesons perpendicular to the beam direction. The sign of this anisotropy is the same as observed in photoproduction [13], but opposite to the  $\eta$  production with pion beams [14]. Using the idea of the vector dominance model, where the photon is coupling to the proton- $\eta$  vertex by an intermediate vector meson, this is a hint for a dominant vector meson exchange in this energy region. A more detailed interpretation of these data shows a dominant exchange of  $\rho$  vector mesons [5] with a destructive  $\rho/\pi$  interference. The sign of the anisotropy should be opposite if  $\pi$  exchange were dominant.

<sup>a</sup> e-mail: Ingo.Froelich@exp2.physik.uni-giessen.de

<sup>b</sup> Present address: DAPNIA/SPhN, CEA Saclay, France.

<sup>c</sup> Present address: Syngenio AG, Stuttgart

<sup>d</sup> Present address: LPHNHE, Ecole Polytechnique 91128 Palaiseau, France.

<sup>e</sup> Present address: Temple University, Philadelphia, PA, USA.

<sup>f</sup> Present address: Paul Scherrer Institut, Villigen, CH-5232.

<sup>g</sup> Present address: Motorola Polska Software Center, Kraków, Poland.

<sup>h</sup> Present address: d-fine GmbH, Eschborn.

In this report, angular distributions of the exclusive reaction  $pp \rightarrow pp\eta$  are presented, which have been measured with the DISTO-Spectrometer at higher energies. First, an overview of the apparatus and the data analysis techniques are given. In the second part, the measured angular distributions of the  $\eta$  as well as the of recoiling  $pp$  system are shown.

## 2 Experimental setup and analysis steps

The DISTO magnetic spectrometer [15] was located at the SATURNE II accelerator. Proton beams with kinetic energies of 2.15 GeV, 2.50 GeV and 2.85 GeV were directed to a liquid hydrogen target. The relevant components of the detector for the results presented here were a large dipole magnet which covered the target, two sets of multi-wire proportional chambers (MWPC) mounted outside the magnetic field and an array of water Čerenkov detectors, which allowed a separation of protons and pions over a large momentum range. The large solid angle of the detector allowed final states with four charged particles to be measured. Various kinematically complete reactions have been investigated simultaneously under the same conditions of four charged particles in the final state, *e.g.*,  $ppK^+K^-$ ,  $pp\pi^+\pi^-(\pi^0)$  and  $pKY$ ,  $Y = \Sigma, \Lambda$  [16–18].

The exclusive  $\eta$  production has been observed via the reaction  $pp \rightarrow pp\eta \rightarrow pp\pi^+\pi^-\pi^0$  ( $\eta \rightarrow \pi^+\pi^-\pi^0$  branching ratio: 23% [19]). The momentum of each track has been calculated using the hit pattern information of the MWPC. The four-momentum vectors were determined by assigning a mass hypothesis ( $p$  or  $\pi^+$ ) to the positively charged tracks. A  $\chi^2$ -test was applied to the measured three-momenta and Čerenkov light outputs to find the best assignment of the positive tracks to the  $pp\pi^+$  hypothesis. Furthermore, a requirement of  $\chi^2_{\text{best}} < 3$  has been used to suppress events from other reactions (*e.g.*,  $pp \rightarrow pK\Lambda \rightarrow ppK\pi$ ).

After the identification of all four charged particles in the final state, energy and momentum conservation can be used to reconstruct the invariant mass  $M_X^{\text{inv}}$  and missing mass  $M_X^{\text{miss}}$  of specific particle combinations  $X$ . To select the reaction  $pp\pi^+\pi^-\pi^0$  versus other reaction channels with  $pp\pi^+\pi^-$  in the final state a missing  $\pi^0$  has been required with the conditions  $0.002 \text{ GeV}^2/c^4 < (M_{pp\pi^+\pi^-}^{\text{miss}})^2 < 0.037 \text{ GeV}^2/c^4$  and  $(M_{\pi^+\pi^-}^{\text{inv}})^2 < (M_{pp}^{\text{miss}})^2$ . A further suppression of background and gain in momentum resolution have been achieved by refitting the four tracks with the additional constraint that  $M_{pp\pi^+\pi^-}^{\text{miss}} = M_{\pi^0}$  [17].

To evaluate the acceptance of the detector, Monte Carlo simulations have been used, which were processed through the same analysis chain as the measured data. The simulations indicate a very low acceptance of the apparatus for the  $\eta$  produced in the backward hemisphere in the CM frame. However, since the initial system consists of two identical particles, a reflection symmetry about  $\theta^{\text{CM}} = 90^\circ$  exists, thus the backward data are redundant for the cross-section determination. In the forward hemi-

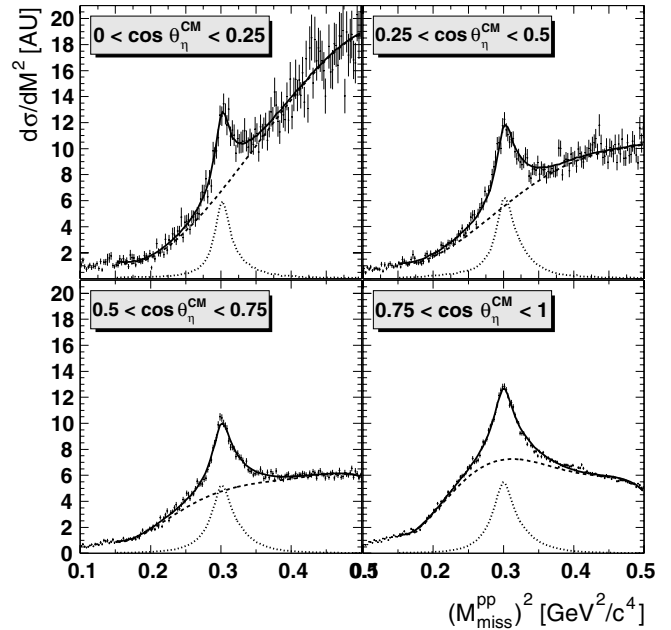


**Fig. 1.** Proton-proton missing-mass squared for 4 different  $\cos \theta_\eta^{\text{CM}}$ -bins (2.85 GeV data) before absolute normalization. Dotted line:  $\eta$  line shape from Monte Carlo simulation. Dashed line: background (polynomial of 6th order). Solid line: signal plus background. Both data and simulation have been corrected for acceptance in the  $\eta$  invariant mass region.

sphere the detector acceptance was found to be non-zero in every bin over the full kinematically allowed region, thus eliminating the need for any model-dependent extrapolations of the cross-section into unmeasured regions of phase space.

The kinematically allowed phase space of the three-body  $pp\eta$  final state has been divided into 4-dimensional kinematic bins. We have chosen the invariant masses  $M_{p_1\eta}^{\text{inv}}$ ,  $M_{p_2\eta}^{\text{inv}}$  and three Euler angles  $\theta_\eta^{\text{CM}}$ ,  $\phi_\eta^{\text{CM}}$ ,  $\psi_{pp}^{\text{CM}}$  as the degrees of freedom, where symmetry reasons ensure that the  $\phi_\eta^{\text{CM}}$  distribution must be isotropic. The efficiency correction factor was determined for each bin separately by dividing the number of generated  $pp\eta$  events by the number of reconstructed events in the corresponding acceptance bin. The data presented below have been corrected on an event-by-event basis via this weighting factor. For a detailed discussion see [18].

The data which has been selected by all conditions still contain background, mostly from non-resonant  $\pi^+\pi^-\pi^0$  production. A  $\chi^2$  minimization routine has been applied to a parametrization of the background and signal. The background has been parameterized by a 6th-order polynomial. The line shape of the  $\eta$  signal was derived from Monte Carlo simulation for each individual bin of the angular distributions. Figure 1 shows the  $pp$  missing-mass distribution (2.85 GeV data) for four ranges of  $\cos \theta_\eta^{\text{CM}}$ , which is the polar angle of the  $\eta$ -meson with respect to the beam direction in the  $pp\eta$  CM system.

Due to the large systematic uncertainty of the beam current normalization, we did not measure the total cross-section of the  $pp \rightarrow pp\eta$  reaction. However, the total

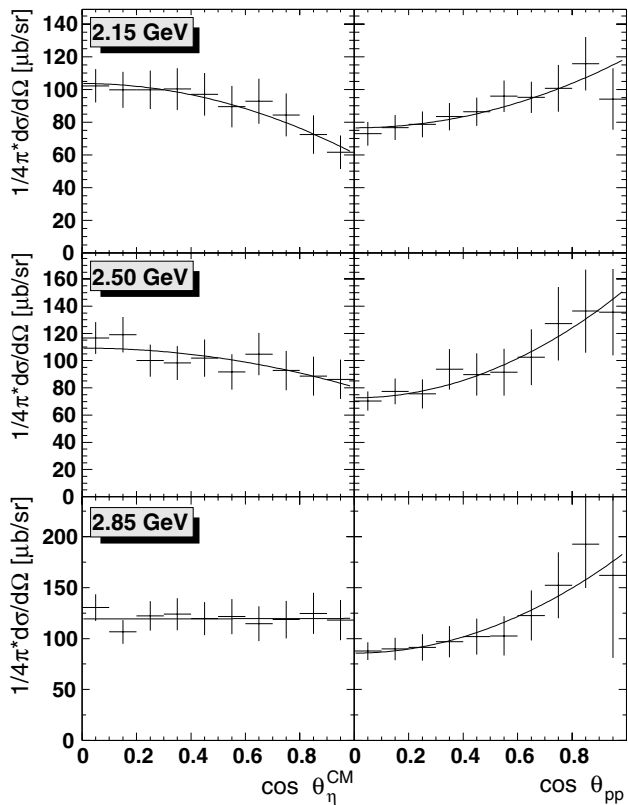


**Fig. 2.** Angular distributions of the  $\eta$  with respect to the beam direction (left column) and of the  $pp$  system in the  $pp$  rest frame (right column). The data have been fitted with the first two even Legendre polynomials. The error bars include both statistical and systematical uncertainties. The histograms on the right side have been scaled by a factor of  $\frac{1}{2}$  since  $\cos \theta_{pp}$  is only defined between 0 and 1.

cross-section of  $pp \rightarrow pp\eta$  is known from many other experiments, allowing us to obtain the absolute normalization of the angular distributions, as shown in [18]. Following the same procedure, we used  $90 \pm 20 \mu\text{b}$ ,  $100 \pm 30 \mu\text{b}$  and  $120 \pm 40 \mu\text{b}$  for the  $T_{\text{beam}} = 2.15 \text{ GeV}$ ,  $2.50 \text{ GeV}$  and  $2.85 \text{ GeV}$  data, respectively. Since the absolute normalization enters only as a global scale, the related error bars have not been included in the errors of the individual bins in the presented angular distributions.

However, each bin of the angular distributions has an individual error due to systematic effects, which are dominated by the acceptance correction and background subtraction. To evaluate those bin-by-bin errors, both the statistical error from the minimization routine and the bin-by-bin systematical error have been taken into account. The systematic error has been obtained by comparing background fits with similar  $\chi^2$  values but different conditions on both the polynomials and the signal shape and included in the angular differential cross-sections presented in this work.

### 3 Results

The differential cross-section has been evaluated as a function of  $\cos \theta_{\eta}^{\text{CM}}$  and  $\cos \theta_{pp}$ , as shown in fig. 2. Here,

**Table 1.** Contribution  $c_2$  of the 2nd Legendre polynomial.

Beam energy	Excess energy	$c_2(\eta)$	$c_2(pp)$
2.15 GeV	324 MeV	$-0.33 \pm 0.20$	$0.31 \pm 0.06$
2.50 GeV	412 MeV	$-0.19 \pm 0.15$	$0.38 \pm 0.07$
2.85 GeV	554 MeV	$-0.01 \pm 0.10$	$0.50 \pm 0.06$

$\theta_{pp}$  is the polar alignment of the  $pp$  system in the  $pp$  rest frame with respect to the beam axis. The observables have been divided into 10 bins, for each bin the yield has been extracted by fitting and subtracting the background. Both angular distributions have been fitted with the sum of the first two even Legendre polynomials  $\frac{d\sigma}{d\Omega} \propto L_{0,2}(\cos \theta) = c_0[1 + c_2 L_2(\cos \theta)]$  to evaluate the contributions of  $c_0$  and  $c_2$ . The  $c_2$  parameters at the different beam energies are compared in table 1. These results indicate an anisotropy of the produced  $\eta$ -meson perpendicular to the beam direction at 2.15 GeV, which is smaller for the 2.50 GeV data and vanishes for the highest energy. The  $c_2$  contribution of the protons increases with the beam energy. The inclusion of Legendre polynomials of higher order were not necessary to describe the data points.

In conclusion, we have measured the angular distribution in the reaction  $pp \rightarrow pp\eta$  with the DISTO spectrometer at beam energies of 2.15 GeV, 2.50 GeV and 2.85 GeV. The anisotropies of the  $\eta$ -meson polar angle at 2.15 GeV gradually vanishes at larger beam energies. This behaviour should be considered in upcoming theoretical approaches together with the new near-threshold data from COSY [20] with higher statistics in one framework.

We acknowledge the work provided by the SATURNE II accelerator staff and technical support groups in delivering an excellent proton beam and assisting this experimental program. This work has been supported by CNRS-IN2P3, CEA-DSM, NSF, INFN, KBN (5P03B14020) and GSI.

### References

1. J.-F. Germond, C. Wilkin, Nucl. Phys. A **518**, 308 (1990).
2. T. Vetter, A. Engel, T. Biró, U. Mosel, Phys. Lett. **263**, 153 (1991).
3. J.M. Laget, F. Wellers, J.F. Lecomte, Phys. Lett. B **257**, 254 (1991).
4. A. Sibirtsev, W. Cassing, Few-Body Systems Suppl. **99**, 1 (1999).
5. G. Fäldt, C. Wilkin, Phys. Scr. **64**, 427 (2001).
6. E. Chiavassa *et al.*, Phys. Lett. B **322**, 270 (1994); E. Chiavassa *et al.*, Phys. Lett. B **337**, 192 (1994).
7. A.M. Bergdolt *et al.*, Phys. Rev. D **48**, R2969 (1993); F. Hibou *et al.*, Phys. Lett. B **438**, 41 (1998).
8. A. Khoukaz *et al.*, Nucl. Phys. A **663** & **664**, 565c (2000); J. Smyrski *et al.*, Phys. Lett. B **474**, 182 (2000).
9. Roderburg *et al.*, Acta Phys. Pol. B **31**, 2299 (2000).
10. H. Calén *et al.*, Phys. Lett. B **366**, 39 (1996).
11. H. Calén *et al.*, Phys. Rev. C **58**, 2667 (1998).
12. H. Calén *et al.*, Phys. Lett. B **458**, 190 (1999).
13. B. Krusche *et al.*, Phys. Rev. Lett. **74**, 3736 (1995).

14. W. Deinet *et al.*, Nucl. Phys. B **11**, 495 (1969).
15. F. Balestra *et al.*, Nucl. Instrum. Methods **426**, 385 (1999).
16. F. Balestra *et al.*, Phys. Rev. Lett. **81**, 4572 (1999).
17. F. Balestra *et al.*, Phys. Lett. B **491**, 29 (2000).
18. F. Balestra *et al.*, Phys. Rev C **63**, 024004 (2000).
19. D.E. Groom *et al.*, Eur. Phys. Jour. C **15**, 1 (2000).
20. P. Moskal *et al.*, PiN Newslett. **16**, 367 (2002), nucl-ex/0110018; The COSY-TOF Collaboration (M. Abdel-Bary *et al.*), Eur. Phys. J. A **16**, 127 (2003), nucl-ex/0205016.